

Weak pinning: Surface growth in presence of a defect

F. Slanina^{a,b,1} and M. Kotrla^{a,2}

^a *Institute of Physics, Academy of Sciences of the Czech Republic,
Na Slovance 2, CZ-18040 Praha, Czech Republic*

^b *Center for Theoretical Study, Jilská 1, CZ-11000 Praha, Czech Republic*

Abstract

We study the influence of a point defect on the profile of a growing surface in the single-step growth model. We employ the mapping to the asymmetric exclusion model with blockage, and using Bethe-Ansatz eigenfunctions as a starting approximation we are able to solve this problem analytically in two-particle sector. The dip caused by the defect is computed. A simple renormalization group-like argument enables to study scaling of the dip with increasing length of the sample L ; the RG mapping is calculated approximately using the analytical results for small samples. For a horizontal surface we found that the surface is only weakly pinned at the inhomogeneity; the dip scales as a power law L^γ with $\gamma = 0.58496$. The value of the exponent agrees with direct numerical simulations of the inhomogeneous single-step growth model. In the case of tilted surfaces we observe a phase transition between weak and strong pinning and the exponent in the weak pinning regime depends on the tilt.

Key words: Growth; Asymmetric exclusion model; Pinning

PACS: 05.40.+j; 81.10.Aj; 61.72.Bb

1 Introduction

There has been much activity in the field of surface growth in the last period [1,2]. Some problems are now rather well understood, nevertheless, many questions still remain open or not completely clarified. One of them is the effect of defects on growth. In particular, we have in mind a defect which persists

¹ e-mail: slanina@fzu.cz

² e-mail: kotrla@fzu.cz

during the growth and makes the growth inhomogeneous. This problem is relevant for various physical situations. For example, 1+1 dimensional epitaxial growth (one-dimensional substrate and one dimension in the direction of growth) of steps on vicinal surfaces when there is a line defect on the terrace in the growth direction. Growth becomes inhomogeneous, the growth velocity at the defect can be lower (the moving step edge is pinned to the defect) or higher (the defect causes an excess of incorporated particles) than averaged velocity of the homogeneous step edge. An impurity floating on the growth front can have similar effect. In the case of 2+1 dimensional growth on a substrate with a defect (for example a dislocation) the defect is replicated in the grown material and makes the growth inhomogeneous. Still another situation is growth of a two-component material forming two domains separated by a domain wall; growth rate at the domain wall is different from growth rate within domains [3]. Epitaxial growth in these situations was so far little studied theoretically, although it is of great practical importance. Nevertheless, similar problems were investigated in different contexts [4–9].

From the statistical-mechanical point of view the central problem is the existence and the character of pinning - depinning transition. The lack of deposition may result in a dip of depth d located at the defect. The growing surface may be pinned, if d scales linearly with the sample size L , or it may be depinned, if d remains finite when the sample size goes to infinity. However, the dip may scale as a power of L , $d \sim L^\gamma$. To distinguish between different situations we shall call the case with $\gamma = 1$ *strong pinning*, and the case $0 < \gamma < 1$ *weak pinning*. The situation when $\gamma = 0$ corresponds either to depinning, if $\lim_{L \rightarrow \infty} d = \text{const} < \infty$, or to various types of logarithmic pinning, like $d \sim (\log L)^\nu$ with positive exponent ν .

Several authors investigated the problem of pinning of growing interfaces through various formulations. Wolf and Tang [4] studied inhomogeneous growth analytically using the growth equation proposed by Kardar, Parisi and Zhang (KPZ) [10]. They found that depending on the sign of the coefficient λ in front of the non-linear term in the KPZ equation there is different behaviour of the surface profile with the size L of the sample for the lack and for the excess of deposition at the defect. For $\lambda > 0$, extra deposition at the defect site leads to a pile of amplitude d increasing linearly with L , whereas the lack of deposition produce a groove of depth d , increasing logarithmically, $d \sim \log L$. For $\lambda < 0$, linear and logarithmic dependence are interchanged.

Kandel and Mukamel [5] performed numerical simulations of 1+1 dimensional polynuclear growth model with a defect. They observed a defect-induced phase transition when changing the strength of the defect, manifested by the change of the dependence of the dip, d , on the system size. They found that d scales as $d \sim L^\gamma$, with $\gamma = 1$ in the strong-defect phase, while $\gamma < 1$ for weak defect phase. In further investigation, a mean-field description of the phase transition

was used [8] and the mean-field value of the exponent γ in the weak defect phase was found to be $\gamma = 0$.

Tang and Lyuksyutov [6] investigated the problem in mathematically equivalent formulation as localization of a directed polymer in disordered medium. They found that there is no depinning transition in 1+1 dimensions for a line defect³ and in 2+1 dimensions for a plane defect, while depinning occurs for a line defect in 2+1 dimensions. This finding is not in contradiction with the results of [5], because in [6] the short-time regime $L \gg t^\zeta$ is observed, where the weak pinning cannot be distinguished from strong pinning.

The problem of growth in the single-step model is equivalent to diffusion in the asymmetric exclusion model [7], where the defect corresponds to a blockage. Such a situation was already studied analytically and some results on the nature of the impurity-induced phase transition are available. They deal with the presence of a strongly pinned phase. The matrix technique developed by Derrida *et al.* [7] for studying the asymmetric exclusion model with open boundary conditions was used in the case of mobile impurity in the medium, observing a phase transition when changing the strength of the impurity [11].

Using Bethe Ansatz it was also argued in favour of the existence of the phase transition induced by a point defect [12]. The pinning-depinning transition corresponds to the phase transition characterized by condensation of particles. The exact analysis of small systems ($L \leq 4$) accompanied by the use of Padé approximants [13] gives some rigorous bounds on the region of strongly pinned phase. However, the possibility of the phase transition to the weak pinning regime remained open.

To our knowledge, the case of weak pinning was not explicitly considered in the existing literature and none of available calculations yields reasonable estimate of the exponent γ in the weakly pinned phase, even though the matrix technique should in principle be able to give exact solution and the generalized Bethe Ansatz for complicated boundary conditions seems promising [14]. At present it is not clear under which conditions the weakly pinned phase with $0 < \gamma < 1$ exists and what is the value of γ .

In this paper we show the existence of weak pinning and present the calculations of the exponent γ in 1+1 dimensional single-step model of inhomogeneous growth. We use an approach combining Bethe Ansatz and renormalization-group argument. We also present results of numerical simulations confirming the predicted exponent.

³ In the context of directed polymers the term line defect corresponds to what we shall call point defect in the growth model or asymmetric exclusion model terminology.

The article is organized as follows. In section 2 we describe the growth model considered, and give the definition of the dip for the surface of an arbitrary orientation. In section 3 the one particle solution is described explicitly. The latter result is used in section 4 for construction of two-particle states. Section 5 contains our main results, both analytical and numerical, and the last, sixth section is devoted to discussion of the results.

2 Growth model with a local defect

In numerical simulations of surface growth, solid-on-solid (SOS) models are often employed because the surface can be simply described by a single height function $h(x)$ of the substrate coordinate x . In most of numerical studies of inhomogeneous growth, so-called restricted solid-on-solid (RSOS) models with the additional constraint on the height difference of the neighbouring sites were used. The direct consequence of the constraint is that the number of possible configurations is finite. The RSOS models are rather well understood in the case of homogeneous growth [1]. The simplest one of these models is the single-step model with the height difference being only $+1$ or -1 . This class of models is particularly suitable for numerical as well as analytical approaches. In 1+1 dimensions an exact solution is known, using the Bethe Ansatz [15].

We consider an inhomogeneous 1+1 dimensional single-step growth model. The state of the system is described by an array $h(x)$, $x = 0, 1, 2, \dots, L$ of integers, which represent the height of the surface at the site x with the constraint $|h(x+1) - h(x)| = 1$ which enables representation of the state of the surface using Ising spin variables $\sigma(x)$ defined by $\sigma(x) = h(x) - h(x-1)$. We impose cyclic boundary conditions. In terms of the spin variables they read $\sigma(0) = \sigma(L)$, while for the height variables they fix the difference $h(0) - h(L)$, *i. e.* the global tilt, constant during the growth. We consider only pure growth (no evaporation). Growth is possible only at a growth site x which obeys the condition $\sigma(x) = -1, \sigma(x+1) = 1$. The deposition of a particle results in the change of the configuration: $h(x) \rightarrow h(x) + 2$ *i. e.* $\sigma(x) \rightarrow -\sigma(x), \sigma(x+1) \rightarrow -\sigma(x+1)$. The inhomogeneity is introduced by the change of the rate for deposition on one fixed site. We suppose the deposition rate at a growth site $x \neq x_0$ to be equal to 1, and the deposition rate at a growth site on the defect site $x = x_0$ to be $1 - \alpha$. The variable α denotes the strength of the defect. The value $\alpha = 1$ corresponds to total inhibition of growth at the defect, *i. e.* to maximum possible pinning; due to the single-step constraint the surface profile evolves to a triangular shape in which it remains frozen.

Let $h(x, t)$ be the surface height at time t . To measure the pinning of the

surface with an arbitrary tilt $(h(L, t) - h(0, t))/L$, we introduce the quantity

$$\Delta\bar{h}(x) = \frac{1}{T} \sum_{t=t_0}^{t_0+T} \left(h(x, t) - h(0, t) - x \frac{h(L, t) - h(0, t)}{L} \right), \quad (1)$$

which we call averaged height difference. It is the height averaged over (long) time interval T with the steady increment of the height and the tilt of the surface subtracted. If there were no defect, the averaged height difference would be zero. The defect at x_0 introduces an inhomogeneity into the system and $\Delta\bar{h}(x)$ may depend on position. We define the dip at the defect site as

$$d = \frac{1}{L} \sum_{x=1}^L \Delta\bar{h}(x) - \Delta\bar{h}(x_0). \quad (2)$$

The surface is pinned, if d/L remains finite in the thermodynamic limit, $L \rightarrow \infty$. It seems natural to say that the surface is depinned if $d/L \rightarrow 0$. In this sense, $\lim_{L \rightarrow \infty} \frac{d}{L}$ is the order parameter of the pinning transition. However, d/L may converge to zero in the thermodynamic limit even if $d \sim L^\gamma$ with $0 < \gamma < 1$. The dip blows up, but more slowly than the length of the sample, therefore we call this situation *weak pinning* with exponent γ .

The dynamics of the system has the following conservation law. The sum of all spin variables, $S = \sum_x \sigma(x)$ does not change during the growth. S should be understood as the average orientation of the surface, $S = h(L) - h(0)$, fixed by the boundary conditions. The single-step model is mapped to the asymmetric exclusion model if we consider down spins as particles and up spins as unoccupied sites. In the language of asymmetric exclusion model, the corresponding conserved quantity is the number of particles $n = (L - S)/2$. The particle density $\rho = n/L$ is $1/2$ for horizontal and $\rho \neq 1/2$ for tilted surface.

The situation corresponds to directed diffusion of n hard core particles on a line. At each time step, each particle can remain in the original position or jump to its right next neighbour site, provided it is unoccupied. The jumping rate from the site x_0 to $x_0 + 1$ is $1 - \alpha$, while the jumping rate from x to $x + 1$ for $x \neq x_0$ is 1.

The conservation law facilitates the exact solution of the system. The Bethe Ansatz solution [15] starts with writing the master equation for the probabilities of all possible configurations. The set of all configurations can be divided into sectors according to number of particles. For each number of particles n , the master equation

$$\dot{p}(x_1, x_2, \dots, x_n) = \sum_{\{x'\}} T_{n\{x\}\{x'\}} p(x'_1, \dots, x'_n) \quad (3)$$

is solved independently. Here, the variables x_1, \dots, x_n describe positions of the particles and $p(x_1, \dots, x_n)$ is probability of finding the particles in the specified spatial configuration. The spectrum of the n -particle transition matrix T_n contains all information on the dynamics of the system. The solution for arbitrary n is still not known. We shall present exact solution for $n = 1, 2$.

3 One-particle problem

In the case of a single diffusing particle the solution is quite easy. For $n = 1$ the master equation has a very simple form

$$\begin{aligned} \dot{p}(x) &= p(x-1) - p(x) & , \text{ for } x \neq x_0, x \neq x_0 + 1 & , \\ \dot{p}(x_0) &= p(x_0-1) - (1-\alpha)p(x_0) & , \\ \dot{p}(x_0+1) &= (1-\alpha)p(x_0) - p(x_0+1) & . \end{aligned} \tag{4}$$

We can solve it by finding the (right) eigenvectors of the transfer matrix T_1 in the one-particle sector. The eigenvectors are parametrized by a complex number ζ . As we shall see, also the left eigenvectors are useful, so we determine both of them.

We write

$$\sum_y T_{1xy} \pi_\zeta(y) = \lambda_\zeta \pi_\zeta(x) \tag{5}$$

for the right eigenvectors and

$$\sum_x \pi_\zeta^T(x) T_{1xy} = \lambda_\zeta \pi_\zeta^T(y) \tag{6}$$

for the left ones. The left and right eigenvectors for different λ_ζ are mutually orthogonal.

We look for the solution in the form $\pi_\zeta(x) = A\zeta^x$ for $x < x_0$ or $x > x_0$, where A may be different in the regions $x < x_0$ and $x > x_0$. We find easily

$$\begin{aligned} \pi_\zeta(x) &= \zeta^x & , \text{ for } x < x_0 & , \\ \pi_\zeta(x_0) &= \zeta^{x_0} \frac{1}{1-\alpha\zeta} & , \\ \pi_\zeta(x) &= \zeta^x \frac{1-\alpha}{1-\alpha\zeta} & , \text{ for } x > x_0 & , \end{aligned} \tag{7}$$

and similarly for the left eigenvectors

$$\begin{aligned}\pi_{\zeta}^T(x) &= \zeta^{-x} \quad , \text{ for } x \leq x_0 \quad , \\ \pi_{\zeta}^T(x) &= \zeta^{-x} \frac{1-\alpha\zeta}{1-\alpha} \quad , \text{ for } x > x_0 \quad .\end{aligned}\tag{8}$$

The corresponding eigenvalue is $\lambda_{\zeta} = \zeta^{-1} - 1$. The stationary solution $p_s(x)$ of the master equation is the eigenvector with zero eigenvalue, *i.e.* with $\zeta = 1$, normalized so that $\sum_x p_s(x) = 1$. The stationary solution gives immediately the stationary height profile. For $\alpha = 0$, the value of $\Delta\bar{h}(x)$ is zero for all x , whereas for $\alpha > 0$ we have

$$\begin{aligned}\Delta\bar{h}(x) &= \frac{2\alpha x}{L(L(1-\alpha)+\alpha)} \quad , \text{ for } x < x_0 \quad , \\ \Delta\bar{h}(x) &= \frac{2\alpha(x-L)}{L(L(1-\alpha)+\alpha)} \quad , \text{ for } x \geq x_0 \quad .\end{aligned}\tag{9}$$

Hence the dip at the defect is

$$d(1, L, \alpha) = \alpha \frac{L-1}{L(L(1-\alpha)+\alpha)} \quad .\tag{10}$$

Because there is only one particle, it is obvious that the surface is not pinned; the value of the dip for all α and L is at most 1. So, in order to actually observe the pinning, we should have non-zero density of particles in the thermodynamic limit $L \rightarrow \infty, n \rightarrow \infty$. This requires a substantially different approach.

4 Lattice constant doubling

We apply a scheme similar to the real space renormalization group technique. Suppose we have even number n of particles in the sample of length L , which is also even. The time evolution is governed by the transfer matrix $T_n(\alpha)$. (From now on we shall write explicitly the dependence of the transfer matrix on α). The presence of the defect of strength α results in a dip $d(n, L, \alpha)$. Taking each pair of neighbour particles as a single object, we have system of $n/2$ effective particles. Their interactions are rather complex, but the fact, that the particles are hard-core, *i.e.* they can not skip one another, is preserved even for the effective particles. The time evolution is no more described by a Markov process governed by some transfer matrix, but by a more general evolution operator $\mathcal{T}_{n/2}(\alpha)$. However, we suppose that we can approximate the dynamics by a Markov process and map the system of $n/2$ effective particles onto

the original system, but with half number of particles and different effective strength of the defect α_2 :

$$\mathcal{T}_{n/2}(\alpha) \rightarrow T_{n/2}(\alpha_2) . \quad (11)$$

The lattice constant of the new system is twice as large, because pairs of particles occupy two original sites, so the length of the rescaled sample is half of the original one. Also the height is rescaled by a factor 2. The procedure roughly corresponds to replacing four atoms deposited independently on the surface by a single “composite” atom made of four original atoms glued together. The dependence of rescaled strength of the defect α_2 on the original α can be computed by equating the dip in the original and rescaled system

$$d(n, L, \alpha) = 2d(n/2, L/2, \alpha_2) . \quad (12)$$

This equation may be understood also as the requirement of the equality of deposited mass in the original system and the rescaled system.

A justification for the doubling procedure may be provided *a posteriori* by the comparison of the whole surface profiles in the original and rescaled systems. If the deviation is small even far from the location of the defect, we can suppose that the pairs of particles actually behave like the original particles, but in rescaled system.

The simplest way for obtaining an approximation for the function $\alpha_2(\alpha)$ is to compute the average height profile for $n = 2$ and the corresponding dip. From (10) and (12) it follows that

$$\alpha_2 = \left(\frac{L^2}{L - 2} \right) \frac{d(2, L, \alpha)}{4 + Ld(2, L, \alpha)} . \quad (13)$$

Fortunately, the $n = 2$ case is soluble exactly. If $\alpha = 0$, the solution is given simply by Bethe Ansatz. The many-particle eigenvector is the linear combination of products of one-particle eigenvectors. However, doing the same for $\alpha \neq 0$ does not work, because the system lacks translational symmetry. But the Bethe Ansatz eigenfunctions p_B may serve as a good starting point for further calculations, because they must obey the equation

$$T_2(\alpha)p_B = \lambda p_B \quad (14)$$

in all cases when both particles are far from the defect. Moreover, if we construct the eigenfunction from the exact one-particle eigenvectors (7), which are calculated for given $\alpha \neq 0$, then the equation (14) will hold even if one of the

particles is at the defect. Only such terms when both particles are at (or near) the defect will disagree. But we may treat the difference as a localized perturbation and solve exactly the equation for the resolvent $G(z) = (z - T_2)^{-1}$.

So, let us start by explicitly writing the eigenvalue equation (14). We define the hopping rate from the site x

$$w_x = 1 - \alpha \delta_{xx_0} . \quad (15)$$

Then, the two-particle eigenvalue equation is

$$\begin{aligned} \lambda p(x, y) &= w_{x-1} p(x-1, y) + w_{y-1} p(x, y-1) \\ &\quad - (w_x + w_y) p(x, y) , \\ \lambda p(x, x+1) &= w_{x-1} p(x-1, x+1) - w_{x+1} p(x, x+1) . \end{aligned} \quad (16)$$

From the cyclic boundary conditions it follows that $p(x, y+L) = p(y, x)$.

We construct the Bethe eigenfunctions

$$p_{B\zeta\omega}(x, y) = \pi_\zeta(x)\pi_\omega(y) + A_B \pi_\omega(x)\pi_\zeta(y) , \quad (17)$$

using the one-particle functions (7). The constant

$$A_B = -\frac{\omega-1}{\zeta-1} \quad (18)$$

is set so that (16) are satisfied far from the defect [15]. For $\zeta = \omega = 1$ we take $A_B = 0$. The corresponding λ is

$$\lambda = \lambda_{B\zeta\omega} = \zeta^{-1} + \omega^{-1} - 2 . \quad (19)$$

The values of ζ and ω are set by the cyclic boundary conditions, resulting in a pair of algebraic equations

$$\begin{aligned} \zeta^L &= -\frac{\zeta-1}{\omega-1} \frac{1-\alpha\zeta}{1-\alpha} , \\ \omega^L &= -\frac{\omega-1}{\zeta-1} \frac{1-\alpha\omega}{1-\alpha} , \end{aligned} \quad (20)$$

which can be solved numerically by standard methods. Together with the solution $\zeta = \omega = 1$ we have $L(L-1)/2$ pairs (ζ, ω) . Each of them determines one of right eigenvectors of some matrix T_{2B} , which differs from T_2 only in

several matrix elements, so we can take T_{2B} as a first approximation to T_2 and treat the difference $T_2 - T_{2B}$ as a perturbation. Let P be matrix whose columns are the Bethe eigenfunctions $p_{B\zeta\omega}(x, y)$ (pairs (x, y) denote rows, pairs (ζ, ω) denote columns). We can write

$$T_{2B} = P^{-1}\Lambda P \quad (21)$$

where Λ is the diagonal matrix with numbers $\lambda_{B\zeta\omega}$ on the diagonal. It is quite easy to find the inverse P^{-1} if $\alpha = 0$. As Bethe functions p_B are exact right eigenvectors of T_2 , the Bethe functions $p_{B\zeta\omega}^T$ constructed by the same procedure from the left one-particle eigenvectors π_ζ^T are exact left eigenvectors of T_2 . Because left and right eigenvectors with different eigenvalues are orthogonal, the matrix composed of properly normalized left eigenvectors is the inverse of P . When $\alpha \neq 0$, the situation is different, but in fact we need to make only a tiny modification.

It can be checked directly (actually we performed the check using Maple V) that the vectors

$$\begin{aligned} p_B^T(x, y) &= \pi_\omega^T(x)\pi_\zeta^T(y) + A_B\pi_\zeta^T(x)\pi_\omega^T(y) \ , \\ &\text{for } (x, y) \neq (x_0, x_0 + 1) \ , \\ p_B^T(x_0, x_0 + 1) &= \frac{1}{1-\alpha} (\omega^{-x_0}\zeta^{-x_0-1} + A_B\zeta^{-x_0}\omega^{-x_0-1}) \end{aligned} \quad (22)$$

are orthogonal to the vectors p_B and so, after proper normalization, they represent rows of the matrix P^{-1} .

As we already said, vectors p_B are considered as nearly exact eigenvectors of T_2 . What we exactly mean is that

$$T_2P = P\Lambda + \Delta \ , \quad (23)$$

where the matrix Δ has only two non-zero rows, corresponding to row indices $a = (x_0 - 1, x_0)$ and $b = (x_0, x_0 + 1)$. (The column indices are the pairs (ζ, ω)). We have explicitly

$$\begin{aligned} \Delta_{a(\zeta, \omega)} &= \alpha(\zeta^{-1} + \omega^{-1} - 1 - \alpha) \frac{\zeta^{-\omega}}{\zeta^{-1}} \frac{(\zeta\omega)^{x_0}}{(1-\alpha\zeta)(1-\alpha\omega)} \ , \\ \Delta_{b(\zeta, \omega)} &= -\alpha(1 - \alpha) \frac{\zeta^{-\omega}}{\zeta^{-1}} \frac{(\zeta\omega)^{x_0}}{(1-\alpha\zeta)(1-\alpha\omega)} \ , \\ \Delta_{a(1,1)} &= \frac{\alpha}{1-\alpha} \ , \\ \Delta_{b(1,1)} &= -\frac{\alpha}{1-\alpha} \ . \end{aligned} \quad (24)$$

The solution is obtained, as soon as we compute the resolvent $G(z) = (z - T_2)^{-1}$. If we define the “unperturbed” resolvent $G^o(z) = (z - P^{-1}\Lambda P)^{-1}$, using elementary matrix algebra we obtain equation

$$G(z) = G^o(z) + G(z)\Delta(z - \Lambda)^{-1}P^{-1} , \quad (25)$$

which we call Dyson equation, taking an analogy from the quantum mechanics.

Let Π be projector to the two-dimensional subspace corresponding to indices a and b and $\bar{\Pi} = 1 - \Pi$ the complementary projector to it. The Dyson equation can be solved within that subspace, because $\Pi\Delta = \Delta$. We obtain

$$\begin{aligned} G(z)\Pi &= G^o(z)\Pi(1 - \Delta(z - \Lambda)^{-1}P^{-1}\Pi)^{-1} \\ G(z)\bar{\Pi} &= G^o(z)\bar{\Pi} + G^o(z)\Pi(1 - \Delta(z - \Lambda)^{-1}P^{-1}\Pi)^{-1} \times \\ &\quad \times \Delta(z - \Lambda)^{-1}P^{-1}\bar{\Pi} . \end{aligned} \quad (26)$$

Computation of the matrix inverses is very simple, because they involve only matrices 2×2 .

The stationary state is obtained from the resolvent in the $z \rightarrow 0$ limit

$$p_s(x, y) = \lim_{z \rightarrow 0} zG_{(x,y)a}(z) . \quad (27)$$

The column index of the resolvent may be chosen arbitrarily. It corresponds to the fact that stationary state does not depend on initial conditions.

5 Results

We calculated explicitly the two-particle ($n = 2$) stationary state $p_s(x, y)$, defined on the triangle $1 \leq x < y \leq L$ for L ranging from 4 to 32. The figures 1 and 2 show the stationary state for $L = 12$ and $\alpha = 0.1, 0.9$. In both cases, the defect is located at $x_0 = 2$. We can see that for small α the effect of the defect is weaker, but more delocalized in the two-dimensional configuration space (x, y) . The probability is distributed nearly homogeneously, but there is a band of higher probability composed of points which have any of the coordinates x, y equal to x_0 . Large α leads to localization of the eigenfunction around the point $(x_0 - 1, x_0)$; in the latter case a single peak develops which bears nearly all the probability.

These results were further used to calculate the stationary height profile difference $\Delta\bar{h}(x)$ and dependence $\alpha_2(\alpha)$ of the renormalized strength of the defect

on the bare value of α . The figure 3 shows the profiles for $L = 4$ and different α 's. This situation corresponds to horizontal surface ($\rho = 1/2$). In the same Fig. 3 we can also compare the exact $n = 2$ (two-particle) profiles with the effective one-particle ones, calculated for $n = 1$, $L = 2$ and defect strength $\alpha_2(\alpha)$. We can see that the agreement is rather good in the whole range of α , which justifies our doubling procedure. The figure 4 shows the same for $L = 12$. These height profiles are tilted ($\rho < 1/2$) which leads to the asymmetry of the dip. Even in this case we can see good agreement between the exact two-particle profile and the effective one-particle one. However, for small α

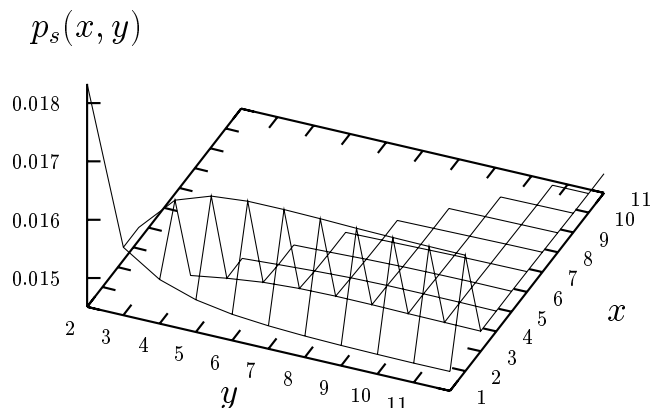


Fig. 1. Stationary state of the two-particle system for $L = 12$ and $\alpha = 0.1$.

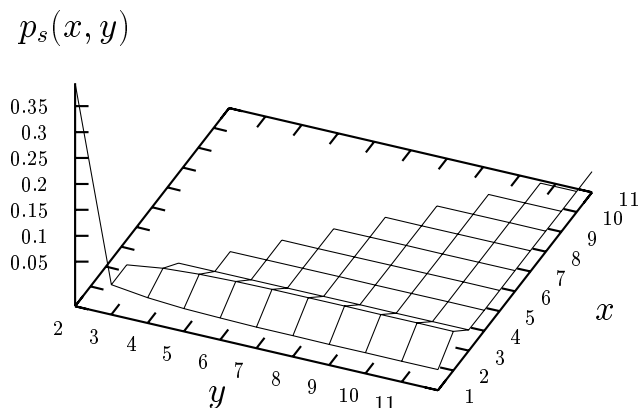


Fig. 2. Stationary state of the two-particle system for $L = 12$ and $\alpha = 0.9$.

and near the defect, the agreement is worse than for horizontal surface.

The key result of our computation is the function $\alpha_2(\alpha)$. In the figure 5, the dependence of $\alpha_2(\alpha)/\alpha$ on α is shown for both horizontal ($\rho = 1/2$) and tilted ($\rho < 1/2$) surfaces.

The physics of pinning is contained in fixed points of the map $\alpha \rightarrow \alpha_2(\alpha)$. There are surely at least two fixed points, namely 0 and 1, corresponding to weak pinning (or depinning) and strong pinning regime, respectively. Their properties may be determined from the quantities

$$\begin{aligned} s_0 &= \lim_{\alpha \rightarrow 0} \frac{\alpha_2}{\alpha} , \\ s_1 &= \lim_{\alpha \rightarrow 1} \frac{1-\alpha_2}{1-\alpha} . \end{aligned} \tag{28}$$

The inequality $s_i < 1 (> 1)$ means that the fixed point $\alpha = i$ is stable (unstable).

Let us comment on the weak pinning regime first. The value of s_0 determines

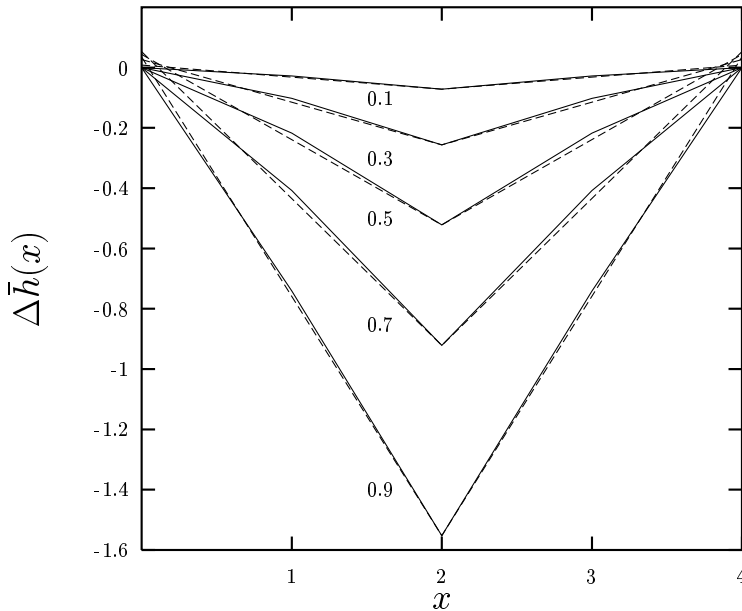


Fig. 3. Stationary height difference for the two-particle system for $L = 4$ and $\alpha = 0.1, 0.3, 0.5, 0.7, 0.9$ (solid lines) together with effective profile of corresponding one-particle system (dashed lines). The numbers close to each full line denote the corresponding α .

the scaling of the dip in the weak pinning regime for $\alpha \rightarrow 0$. The exponent is

$$\gamma = 1 + \frac{\log s_0}{\log 2} , \quad (29)$$

as can be seen from equations (10) and (12).

The values we observe in the Fig. 5 are $1 > s_0 > 0.5$ in all cases, corresponding to weak pinning, $1 > \gamma > 0$, while $s_0 \leq 0.5$ would be signal of depinning (or logarithmic pinning), $\gamma = 0$. Thus, the weak pinning regime is always present.

The most important result is the value of the exponent for horizontal profile. We have observed an interesting result, that for $\rho = 1/2$ it is $s_0 = 3/4$ up to the precision of our numerical procedure (10^{-6}). So, we conjecture, that the exact value of the exponent for horizontal surface and $\alpha \rightarrow 0$ is

$$\gamma = \frac{\ln 3/2}{\ln 2} = 0.58496... \quad (30)$$

This value may be compared directly with numerical simulations.

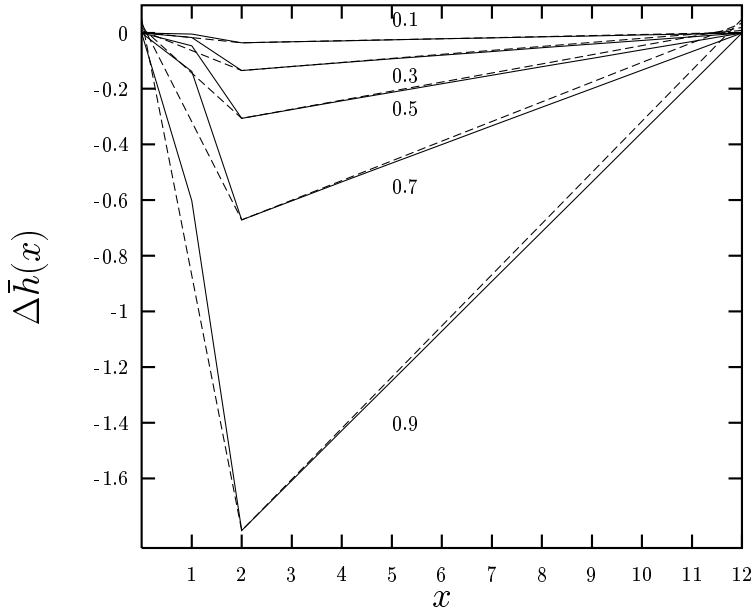


Fig. 4. Stationary height difference, for the two-particle system for $L = 12$ and $\alpha = 0.1, 0.3, 0.5, 0.7, 0.9$ (solid lines) together with effective profile of corresponding one-particle system (dashed lines). The numbers close to each full line denote the corresponding α .

The dependence of s_0 and the corresponding exponent γ on the particle density $\rho = n/L$ is shown in Fig. 6. We can see that the exponent γ decreases smoothly when decreasing the density and seems to approach 0 for $\rho \rightarrow 0$. It reflects the fact, that for zero density there is only finite number of particles on infinite sample and the dip should be also finite. The point at $\rho = 1/2$ does not fit to this smooth dependence. The explanation lies most probably in the different symmetry group of the horizontal surface. (For tilted surfaces, the particle-hole symmetry is broken.)

Let us now turn to the discussion of the phase transition from weak-pinning to strong-pinning regime.

From Fig. 5 we can see, that $\alpha = 0$ is stable fixed point because $s_0 < 1$ for all ρ . On the other hand, we found that the fixed point $\alpha = 1$ is unstable for $\rho = 1/2$ ($s_1 > 1$), but stable for $\rho < 1/2$ ($s_1 < 1$).

The existence of a phase transition for some $\alpha = \alpha_c$ would be signalled by the presence of a third (unstable) fixed point. We may formulate it by saying that $R(\alpha) = \alpha_2(\alpha) - \alpha$ has a root at $0 < \alpha_c < 1$ with positive derivative, $R(\alpha_c) = 0$, $s_c = R'(\alpha_c) > 0$. The critical value α_c separates the weak-pinning (low α) and

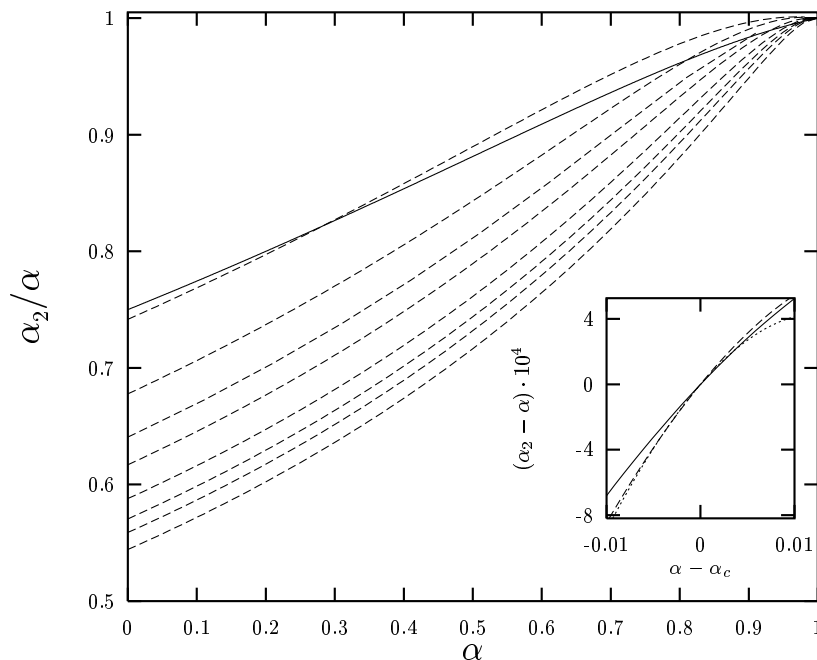


Fig. 5. The α -dependence of the ratio of the effective defect strength α_2 to original α for $\rho = 1/2$ (solid line) and $\rho = 1/3, 1/4, 1/5, 1/6, 1/8, 1/10, 1/12, 1/16$ (dashed lines, from top to bottom). In the inset, detail of the dependence of difference $\alpha_2 - \alpha$ on the distance from the critical point, $\alpha - \alpha_c$, for $\rho = 1/3$ (solid), $\rho = 1/4$ (dashed), $\rho = 1/5$ (dotted).

strong pinning (high α) regimes, corresponding to different scaling of the dip. For $\alpha < \alpha_c$ we have $\gamma < 1$, for $\alpha > \alpha_c$ we have $\gamma = 1$.

For $\rho = 1/2$ we did not find the third fixed point. Instead, the unstable fixed point at $\alpha = 1$ plays its role and we conclude that there is no phase transition for $\alpha < 1$ and we are in the weak pinning regime for all $\alpha < 1$.

For $\rho < 1/2$ we find $\alpha_c < 1$, but very close to 1. The values of α_c are 0.9371, 0.9605, 0.97535 for $\rho = 1/3, 1/4, 1/5$, respectively. The dependence of $R(\alpha)$ on $\alpha - \alpha_c$ near the critical point is shown in the inset in Fig. 5.

Finally, we compare some of our results with numerical simulations. We performed direct Monte Carlo simulations of growth in the inhomogeneous single-step model for horizontal surface, *i.e.*, density $\rho = 1/2$ in asymmetric exclusion model. We measured the dip (2) as the function of the system size L and time t for several strengths of the defect α . When we start from the flat configuration, the dip increases with time and after some time t_{sat} (growing with the system size) the stationary regime is reached. In this regime the dip fluctuates around the characteristic value $d_{\text{sat}}(L) \sim L^\gamma$. We concentrate on the weak defect regime, *i.e.*, small α . In this case fluctuations are very strong and many independent runs are needed to obtain the value of the saturated dip. Results presented in Fig. 7 are averages over 10^4 to 5×10^4 independent runs.

We observed that the slope, *i.e.* exponent γ is slightly decreasing with decreasing α , but it is definitely larger than $1/2$. We calculated exponent γ by fitting the last five points in each curve. Values obtained for $\alpha = 0.05$, $\alpha = 0.1$ and $\alpha = 0.2$ are 0.59 ± 0.03 , 0.61 ± 0.01 and 0.703 ± 0.004 respectively. The

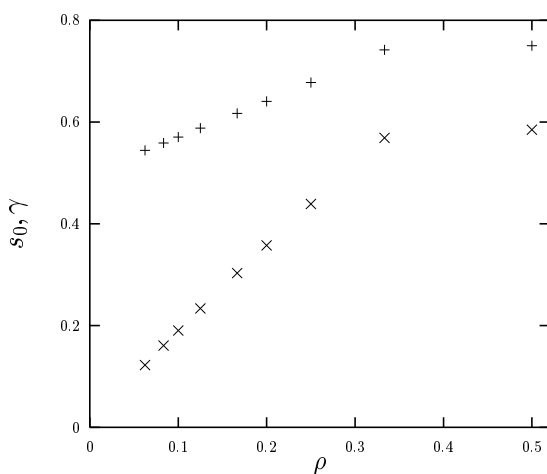


Fig. 6. The slope s_0 at $\alpha \rightarrow 0$ (+) and the exponent γ (x) against the particle density $\rho = n/L$.

value obtained for the lowest value $\alpha = 0.05$ agrees well with the analytical prediction (30), so we conclude that the $\alpha \rightarrow 0$ limit is well described by our analytical calculations.

6 Conclusions and discussion

We solved exactly in a special case the problem of growing interface in presence of a point defect. In the language of asymmetric exclusion model, we obtained the solution for cyclic boundary conditions in the two-particle sector. The solution consists in two steps. At first, using the Bethe-Ansatz eigenfunctions as a basis set, we found that the perturbation becomes localized in the configuration space. Then we solved the Dyson equation exactly by inversion of small matrices. We computed the stationary profile of the surface and determined the dip at the defect. The two-particle result was then employed in a renormalization-group consideration, based on a lattice constant doubling transformation. We obtained the dependence of the effective defect strength α_2 on the original, bare defect strength α . Fixed points of this mapping were identified.

Our main result is the existence of the weak pinning phase and the value of the corresponding exponent. Let us discuss first the situation for a horizontal

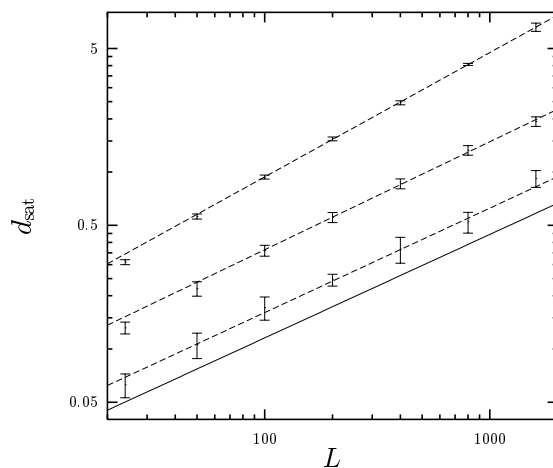


Fig. 7. Saturated dip, d_{sat} , as a function of the system size, L , calculated in the inhomogeneous single-step model for three strengths of the defect $\alpha = 0.05$, $\alpha = 0.1$ and $\alpha = 0.2$ (from bottom to top). The dashed lines are fits to last five points, the slope of the full line corresponds to the value of γ obtained by the analytical solution, eq. (30).

surface ($\rho = 1/2$). We have found just two fixed points: $\alpha = 0$ which is stable, and corresponds to weak pinning of the surface to the defect, $d \sim L^\gamma$ with $0 < \gamma < 1$, and $\alpha = 1$ which is unstable. Hence, from our analytical calculations we obtained for $\alpha < 1$ only the weak pinning phase. The strong pinning regime is limited to a single point $\alpha = 1$. We calculated the exponent γ in the weak pinning phase to be $\gamma = 0.58496$.

We verified the existence of weak pinning by a direct Monte Carlo simulation of the inhomogeneous single-step growth model. For weak defect, α close to 0, we obtained $\gamma = 0.59 \pm 0.03$ in good agreement with the analytical prediction.

The Ref. [4] reports linear dependence of the dip on L , suggesting that $\gamma = 1$. In fact, the authors of [4] state that $d \sim sL$, where s is the slope of the interface at the defect. They use the parameter s as a measure of the strength of the defect. We understand this choice as being dictated by the use of a continuous model (KPZ equation). However, we use different parametrization, namely taking the strength of the defect α as a control parameter. For α fixed, the value of s may depend on L . A direct comparison of Ref. [4] with our results would require measurement of the quantity s , which was not performed in our simulations.

In the case of tilted surfaces, we found that the fixed point $\alpha = 1$ becomes stable, and in addition there is a third, unstable fixed point $0 < \alpha_c < 1$ which corresponds to the phase transition between strong and weak pinning. However, the value of α_c in our calculations is very close to 1.

The absence of phase transition at $\alpha < 1$ for $\rho = 1/2$ is in contradiction with numerical simulations on the inhomogeneous polynuclear growth model [5] as well as with analytical results [12,13]. The most probable reason lies perhaps in the approximation used in calculation of the map $\alpha_2(\alpha)$: instead of working with macroscopic sample with generic length L and particle number n and compare it by the doubling procedure to the sample with length $L/2$ with $n/2$ particles, very small sample, $L = 4$ was used. With such small sample, the influence of boundary conditions may be very strong, deforming the renormalization map $\alpha_2(\alpha)$. Nevertheless, the agreement of the analytical results with simulations in the weak pinning phase shows that for weak defects the method we used works well.

In order to improve the result, it would be necessary to solve the dynamics for a larger number of particles. However, the use of the Bethe-Ansatz eigenfunctions for number of particles larger than two does not lead to localization of the perturbation and Dyson equation cannot be solved exactly by explicit matrix inversion.

It would be of interest to investigate the existence of weak pinning in different inhomogeneous models, in particular one would like to know if the value of

the exponent γ for the strength of the defect going to zero is universal, and eventually if a weak-pinning to depinning transition exists.

Acknowledgments The work was partially supported by the grant No. A 1010513 of the GA AVČR. We wish to thank J. Mašek for many useful discussions.

References

- [1] J. Krug. *Adv. Phys.* **46** (1997) 139 ; T. Halpin-Healy and Y.-C. Zhang, *Phys. Rep.* **254** (1995) 215 ; Paul Meakin, *Phys. Rep.* **235** (1993) 189
- [2] A. C. Levi and M. Kotrla. *J. Phys.: Condens. Matter* **9** (1997) 299 ; A. L. Barabási and H. E. Stanley. *Fractal concepts in surface growth*. Cambridge University Press, Cambridge, 1995 ; M. Kotrla, *Czech. J. Phys.* **42** (1992) 449
- [3] M. Kotrla and M. Předota, *Europhys. Lett.* **39** (1997) 251
- [4] D. E. Wolf and L.-H. Tang, *Phys. Rev. Lett.* **65** (1990) 1591
- [5] D. Kandel and D. Mukamel, *Europhys. Lett.* **20** (1992) 325
- [6] L.-H. Tang and I.F. Lyuksyutov, *Phys. Rev. Lett.* **71** (1993) 2745
- [7] B. Derrida, M. R. Evans, V. Hakim and V. Pasquier, *J. Phys. A: Math. Gen.* **26** (1993) 1493
- [8] D. Kandel, G. Gershinsky, D. Mukamel and B. Derrida, *Physica Scripta* **T49B** (1993) 622
- [9] Z. Torockai and R. K. P. Zia, *Phys. Lett. A* **217** (1996) 97
- [10] M. Kardar, G. Parisi and Y.-C. Zhang, *Phys. Rev. Lett.* **56** (1986) 889
- [11] K. Mallick, *J. Phys. A: Math. Gen.* **29** (1996) 5375
- [12] M. Henkel and G. Schütz, *Physica A* **206** (1994) 187
- [13] S. A. Janovsky and J. L. Lebowitz, *J. Stat. Phys.* **77** (1994) 35
- [14] G. Schütz, *J. Stat. Phys.* **71** (1993) 471
- [15] D. Dhar, *Phase Transitions* **9** (1987) 51 ; L.-H. Gwa and H. Spohn, *Phys. Rev. Lett.* **68** (1992) 725 ; L.-H. Gwa and H. Spohn, *Phys. Rev.* **46** (1992) 844